Origin of helicity-dependent photoconductivity in magnetic and nonmagnetic wires

Atul Pandey,[1,2] Rouven Dreyer,[1] Palvan Seyidov,[1,*] Chris Koerner,[1] Saban Tirpanci,[1] Binoy Krishna Hazra,[2] Stuart Parkin,[2] and Georg Woltersdorf[1,2,†]

[1]*Institute of Physics, Martin Luther University Halle-Wittenberg, Von-Danckelmann-Platz 3, 06120 Halle, Germany*

[2]*Max Planck Institute of Microstructure Physics, Weinberg 2, 06120 Halle, Germany*

(Received 25 May 2022; accepted 16 September 2022; published 18 November 2022)

We study the opto-electric response in metallic wire structures. The aim is to understand the origin of helicity-dependent photoconductivity. For nonmagnetic metals this effect is generally believed to probe spin polarization. Using magnetic wires we show that this method enables background free imaging of spin textures. Analyzing the physical origin we find that the circular dichroism slightly modulates the absorption. The corresponding thermal modulation explains the measured electrical signals. We apply this result to examine the spin Hall effect induced spin accumulation in heavy metals. Here, we show that previously reported results in nonmagnetic wires are well reproducible, but not related to the spin polarization.

DOI: 10.1103/PhysRevB.106.174420

I. INTRODUCTION

Imaging of spin textures is critical for fundamental understanding and technological applications in spin-based electronics [1,2]. These include racetrack and other spin orbit torque memories [3,4]. Such imaging of spin textures can be very challenging in device structures and the observation often relies on electric signals related to magnetoresistive or Hall effects. Alternatively, magnetic circular dichroic effects in the x-ray range (x-ray magnetic circular dichroism) and at optical frequencies (magneto-optic Kerr effect) can be used to detect the magnetic state. Recently, hybrid opto-electric approaches have been introduced. These experiments, based on anomalous Nernst and spin Seebeck effects, demonstrated imaging of the in-plane magnetic texture down to a resolution of a few tens of nanometers [5–7]. Magnetic texture can be controlled by spin polarized charge currents or pure spin currents. Such currents can be generated effectively via the spin Hall effect (SHE) in heavy metals [8–10] or due to spin momentum locking with surface states in topological insulators [11–14]. Typically, the detection of spin currents relies on the magnitude of spin-to-charge conversion effects, which is usually quantified in ferromagnet/normal metal bilayer structures by observing the spin torque exerted on the magnetization [15–17] or by detecting a voltage generated by the inverse SHE [18–20]. However, this approach is fundamentally complicated by unknown parameters such as spin-to-charge conversion efficiency [21] and interface effects [22]. Interface effects may be avoided by manipulating and detecting spin currents within a single material using spin-orbit interaction [23–25]. However, in comparison to the well established optical detection of spin polarization in semiconductors, which is resonantly enhanced in the vicinity of the band gap, such measurements appears to be much more challenging for metals [23,26]. However, in metals only recently spin accumulation was measured by magneto-optical means [27], nonlinear optics [28], and x-ray magnetic circular dichroism [29].

In this article, we explore an opto-electric method that allows for the detection of spin polarization in any conducting material. We use helicity-dependent photoconductivity (HDP) to image the spin polarization in magnetic domains. Here, large HDP signals can be expected due to a sizable magnetic moment. We show that magnetic textures can be imaged opto-electrically with sub-micrometer resolution. In addition, the experiments allow us to quantify the HDP signal and link it to magnetic circular dichroism (MCD). Subsequently, we study current-induced spin polarization in nonmagnetic wires. We find that the spin accumulation induced by SHE is not sufficient to account for the observed HDP signal. We demonstrate that previously reported results can be explained by an optical artifact [30–32].

II. RESULTS WITH MAGNETIC WIRES

First, the magnetic texture of a wire structure is imaged by means of opto-electric microscopy [Fig. 1(a)]. An out-of-plane magnetized sample provides large MCD in the absorption. The magnetic wire structure is defined by dry etching and consists of a Co/Ni/Co stack sputter-deposited on a MgO(001) substrate [33,34]. In the experiment, a magnetic domain wall is trapped in the wire, as verified by polar magneto-optic Kerr microscopy (MOKE) [see Fig. 1(b)]. The sample is illuminated with circularly polarized light. The light's helicity is modulated by means of a photo-elastic modulator (PEM). A dc current is applied to measure the photoresistance. This

*Present address: Leibnitz Inistitut für Kristallzüchtung, Max-Born-Strasse 2, 12489 Berlin, Germany.

†georg.woltersdorf@physik.uni-halle.de

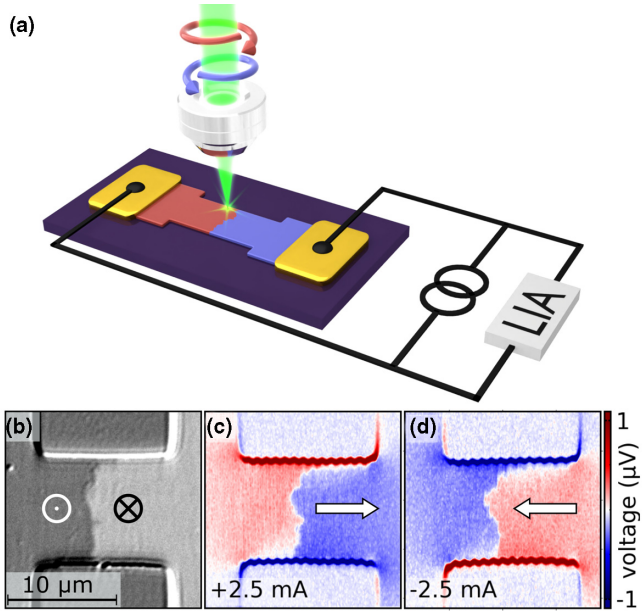

FIG. 1. (a) Measurement geometry of the magnetic sample. While illuminating the sample with a polarization-modulated laser beam, a small dc current (a few mA) is applied. The resulting photovoltage is detected using a lock-in amplifier (LIA) (b) Kerr microscopy image of the out-of-plane magnetized Co/Ni/Co wire. (c) and (d) show the corresponding spatially resolved maps of the helicity-dependent photoresistivity signal of a Co/Ni/Co wire for 2.5 mA and −2.5 mA, respectively. The domain contrast amounts to 400 nV. The signal is detected while the polarization is modulated between σ^+ and σ^-.

resistance is modulated due to absorption-induced heating [see Figs. 1(c) and 1(d)]. The electric signal arising from the magnetic polarization has a magnitude of a few hundred nV and changes its sign as the current direction is reversed. The location of the domain wall observed by means of the HDP signal is consistent with the polar MOKE image. This shows that the signal is caused by the absorption modulation due to MCD and thus provides a probe for spin polarization.

In addition to the expected magnetization-induced contrast, we observe a surprisingly large signal (a few μV) at the edges of the wire. Similar edge effects have been reported in topological materials, such as $BiSbTeSe_2$ [30], Bi_2Se_3 [31], antiferromagnet $IrMn_3$ [32], and heavy metals, such as Pt [31,35]. These signals were attributed to current-induced magnetic moments. The HDP signals were assumed to be caused by magnetic diochroism. Hence these signals are expected to scale with the intrinsic or induced magnetic moment per atom in the sample. Therefore, we compare the HDP signals obtained from the magnetic wires with known magnetic moment (domain contrast) to the signals obtained at the edges of nonmagnetic wires. The domain contrast in the magnetic wire amounts to 100 nV/mA, as shown in Fig. 1.

III. RESULTS WITH NONMAGNETIC WIRES

Next, we opto-electrically measure nonmagnetic metallic wires, as depicted in Fig. 2, exhibiting different signs and magnitudes of the spin Hall angle (SHA). Specifically, we

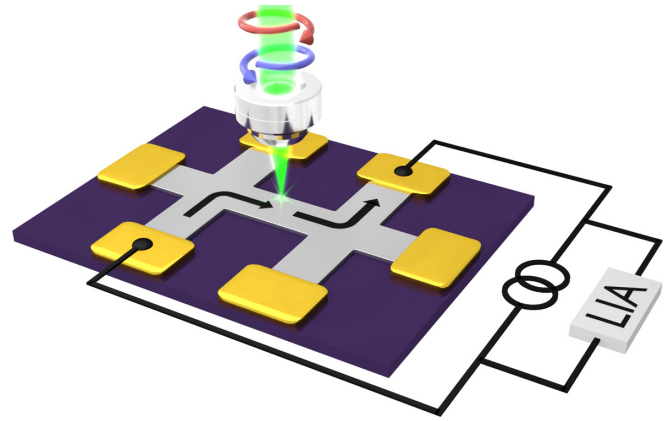

FIG. 2. Measurement geometry for nonmagnetic wire structures. The HDP signal is detected while the optical polarization is modulated between σ^+ and σ^-. Note that the cross shape allows to direct the current around a corner.

investigate wire structures made of Pt (positive SHA), Cu (almost zero SHA), and Ta (negative SHA). Like the magnetic samples discussed above, these wires were also prepared by sputter deposition on MgO(001) substrates. Figure 3(a) shows scanning HDP maps obtained on a 10 nm thick Pt wire with an applied current of ±8 mA. The photo-resistive signal observed on the edges of the wire reverses sign between the left and right edge and with current direction. Its amplitude scales linearly with applied current and laser power [36]. These findings reproduce the results of Liu *et al.* [31]. At the edges of the Pt wire the signal amplitude amounts to 900 nV/mA (compared to 100 nV/mA for the magnetic contrast). This implies that the total magnetic moment at the edges must be an order of magnitude larger than in the ferromagnet. In typical ferromagnets, a magnetic moment of 1 μ_B per atom is expected. However, based on previous experiments [29] and theoretical considerations, the current-induced moment at the sample surface is expected to be 2×10^{-5} μ_B only [27]. This means that the observed signal due to current-induced spin accumulation is at least five orders of magnitude larger than expected.

Furthermore, the measurement geometry needs to be considered. The short spin diffusion length (on the order of 1 nm for Pt and Ta [37–40]) is two orders of magnitude below the diffraction limited resolution of the microscope (300 nm), adding another two orders of magnitude to the discrepancy. Therefore, we need to explain why the electro-optical signals at the edges of nonmagnetic wires are at least seven orders of magnitude larger than expected.

To understand the true physical origin of the HDP signals in nonmagnetic wires, we analyze their current and material dependence. As one can see from Fig. 3, the sign of the edge signal reverses as the bias current is reversed. This behavior is actually not consistent with SHE for the following reason: current reversal should invert the SHE induced spin polarization as well as the sign of the voltage drop across the wire [cf. Figs. 1(c) and 1(d)] resulting in a signal that does not depend on current direction. Moreover, signals with the same symmetry and sign but different magnitude are observed for Cu [Fig. 3(b)] and Ta [Fig. 3(c)] wires as well. While the

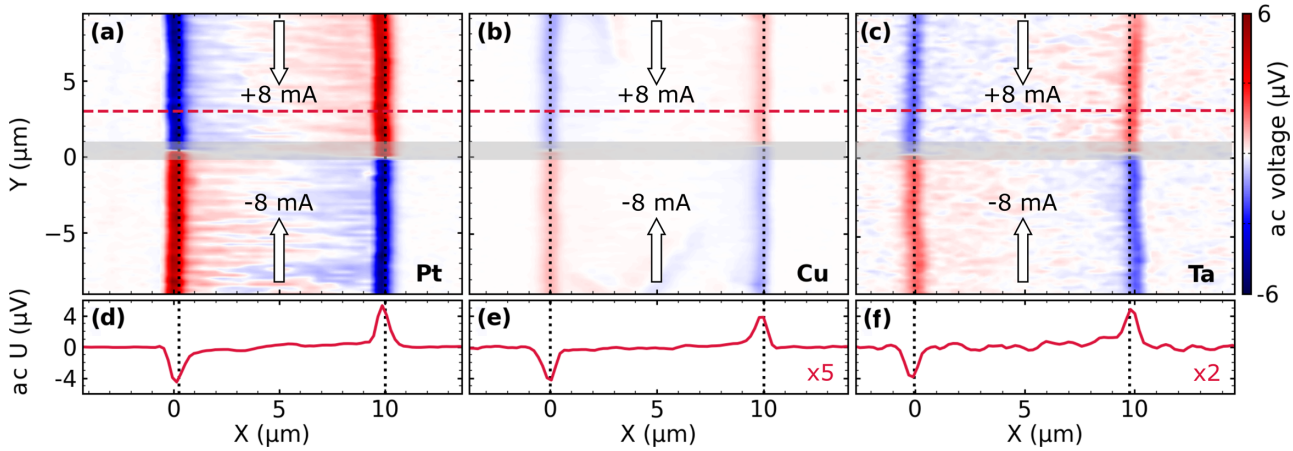

FIG. 3. Photoresistive signal in nonmagnetic wire structures: Spatially resolved maps of the helicity-dependent photoresistivity signal detected at the modulation frequency f_{PEM} in (a) Pt, (b) Cu and (c) Ta wires. In the upper part of the maps a current of 8 mA and in the lower part −8 mA is applied. The grey boxes indicate the switching of current direction. The arrows indicate the current direction and the black, dashed lines show wire edges. (d)–(f) Horizontal line scans obtained at the red dashed line in figures (a)–(c).

different magnitude of the HDP signal can be attributed to different photoconductivity of these materials, the observation of the same signal polarity for Pt and Ta is unexpected since the sign of the SHA in these two materials is opposite. Clearly, the HDP signals at the wire edges are not related to the SHE at all.

To identify the true origin of the edge signals we study their angular dependence. For this, the sample geometry is changed to a cross bar in order to direct the electrical current around a corner. Here, we observe the signal only at the lower vertical edges [Fig. 4(a)] with a two times larger amplitude on the left side than on the right side. Note, that the current flow direction is indicated by the arrows in Fig. 4(a). In contrast, for SHE induced spin polarization, one would expect the same signal amplitude at both, vertical and horizontal lower edges. To verify whether the current density in both wire sections is indeed comparable, we use our photoresistive method to image the current distribution directly. For this, the light intensity is modulated while the photoresistance is recorded [36]. The resulting ac resistance at the light modulation frequency reveals a direct map of the current distribution, as indicated in Fig. 4(b). Obviously, the current densities in horizontal and

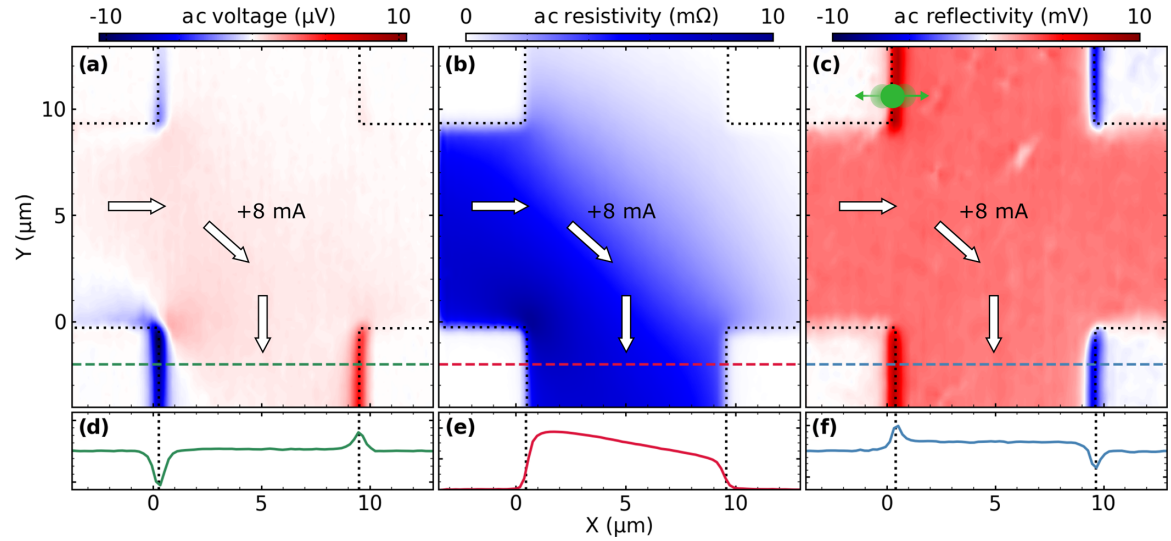

FIG. 4. (a) Helicity-dependent photoresistivity signal detected at the modulation frequency f_{PEM} in a Pt cross section wire for 8 mA current as an ac voltage. (b) Photoresistive detection of the current density in a Pt cross structure using light intensity modulation at $2f_{\mathrm{PEM}}$ and demodulation on of the detected phototresitivity signal at the same frequency. At 8 mA, a photoresistivity of 10 mΩ corresponds to a photovoltage of 80 µV. Panel (c) shows the ac component of the reflectivity demodulated at f_{PEM}. (d), (e), and (f) show line scans at the bottom arm of the cross section for helicity-dependent photoresistivity, current density, and ac reflectivity, respectively.

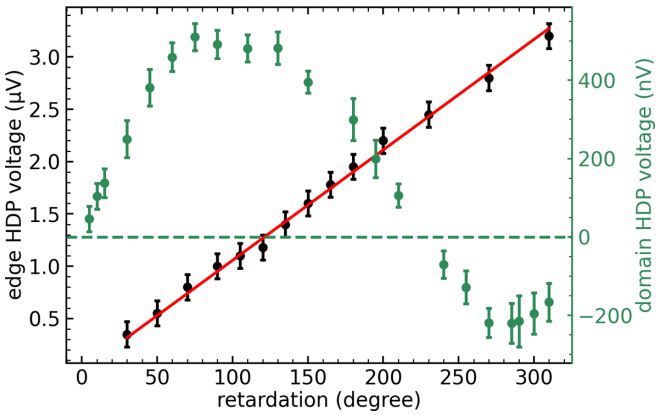

FIG. 5. Magnitude of the HDP signal at the wire edge as a function of retardation amplitude is depicted in black. The difference of the magnetic HDP signal between up and down magnetized domains in Co/Ni/Co wire is shown in green. The error bars represent the rms noise of signal averaged over about 30 seconds in the case of the domain signal ($V_{rms} = 20$ nV) and 2 seconds for the edge signal ($V_{rms} = 150$ nV).

vertical directions are comparable. This means, that the signal scales with the current density but the current alone does not cause the signal at the edges.

The anisotropic behavior of the signal may be explained by a wobbling motion of the focal spot as the helicity is modulated. In this case, different reflectivities of substrate and wire lead to a modulation of the reflected light intensity with the same frequency as the helicity modulation. The obtained map of the ac reflectivity at the polarization modulation frequency indeed contains large signals at the upper and lower wire edges in the vertical direction, as shown in Fig. 4(c). In contrast, no signal is detected at horizontal edges. Again, as for the resistivity, the polarity of the signal changes from the left to the right edge but, in this case, it is not related to the current at all. This result confirms that the focal spot position oscillates in a horizontal direction, as indicated in Fig. 4(c). One can expect that the observed periodic shifting of the focal spot in turn induces a periodic heating of the sample at the wire edges leading to a modulation of resistance at the PEM modulation frequency. This conclusion is consistent with a linear scaling of the HDP edge signal with retardation amplitude, i.e., it does not at all depend on the polarization. In contrast, the magnetic domain signal actually scales periodically with the retardation amplitude as expected for a helicity-dependent signal (see Fig. 5). We conclude that the periodic shifts are caused by the photoelastic modulator. Based on the detailed measurements presented in the Supplemental Material [36], we speculate that the wave fronts of the light are periodically tilted by a very small angle (a few micro rad) due to the excitation of surface acoustic waves in the optical crystal used for the modulation of the polarization. The objective lens subsequently translates these tilts into shifts of the focal spot on the order of 10 nm.

It is possible to distinguish the shift-induced artifact from the true magnetic signal by studying their dependence on the excitation amplitude of the PEM. The phase shift between fast and slow axis of the PEM is generated by a strain wave in a quartz crystal, e.g., for a retardation amplitude of 90° and light linearly polarized at 45° with respect to the PEM axis, a modulation between LCP and RCP results. Based on this, one can expect an oscillatory dependence of the HDP signal as a function of PEM retardation amplitude having extrema of opposite sign at 90° and 270°. Naively one may expect a purely periodic signal as a function of the retardation amplitude for the magnetic case. However, as the retardation depth is increased beyond $\pm\lambda/4$ the light undergoes multiple RCP-to-LCP transitions within one modulation cycle reducing the detectable HDP signal. This decreases the overall signal amplitude that can be measured and results in a damped periodic signal as a function of retardation. Figure 5 shows that while the magnetic signal oscillates with decreasing amplitude as expected, the HDP signal at the edges only scales linearly with retardation. This is expected as it is an optical artifact and caused by the PEM excitation. Most likely, this effect is caused by small periodic tilts of the optical wavefronts due to the strain waves in the PEM resulting in small periodic shifts of laser focal spot.

IV. DISCUSSION AND CONCLUSION

Our results show that, at the wire edge an optical artifact arises that mimics the expected signal from spin Hall induced spin accumulation. Using several PEM systems, as well as the rotation of a quarter wave plate. we have verified that beam shifts in the nm-range during helicity modulation are hardly avoidable. Thus, the measurement geometry must be carefully chosen in order to minimize optical artifacts. As we have demonstrated, it is possible to distinguish between signals induced by spin polarization and optical artifacts by their retardation dependence, see Fig. 5. Hence, there is no fundamental obstacle of using HDP imaging, even in the vicinity of edges. Applying this result to SHE induced spin polarization in heavy metals one needs to consider that here the expected signals are more than at least five orders of magnitude smaller compared to the domain contrast. Considering the noise level of about 100 nV obtained in our experiments, future measurements of SHE induced spin accumulation in photoresistive experiments would require a significantly improved signal- to noise-ratio.

To conclude, we demonstrate that HDP imaging allows for background free imaging of magnetic domain structures. Based on the domain imaging we also clarify the origin of HDP signals at the edges of nonmagnetic wires and attribute them to optical artifacts. In previous studies, such signals were erroneously interpreted as current-induced spin accumulation [30–32,35].

ACKNOWLEDGMENT

Financial support from the German Research Foundation (DFG) through the collaborative research center CRC/TRR 227 (Project ID 328545488, Project B02) is gratefully acknowledged.

[1] S.-H. Yang, K.-S. Ryu, and S. Parkin, Nat. Nanotechnol. **10**, 221 (2015).

[2] T. Higo, H. Man, D. B. Gopman, L. Wu, T. Koretsune, O. M. J. van 't Erve, Y. P. Kabanov, D. Rees, Y. Li, M.-T. Suzuki *et al.*, Nat. Photon. **12**, 73 (2018).

[3] S. S. P. Parkin, M. Hayashi, and L. Thomas, Science **320**, 190 (2008).

[4] L. Liu, C.-F. Pai, Y. Li, H. W. Tseng, D. C. Ralph, and R. A. Buhrman, Science **336**, 555 (2012).

[5] H. Reichlova, T. Janda, J. Godinho, A. Markou, D. Kriegner, R. Schlitz, J. Zelezny, Z. Soban, M. Bejarano, H. Schultheiss, P. Nemec, T. Jungwirth, C. Felser, J. Wunderlich, and S. T. B. Goennenwein, Nat. Commun. **10**, 5459 (2019).

[6] M. Weiler, M. Althammer, F.D. Czeschka, H. Huebl, M.S. Wagner, M. Opel, I.M. Imort, G. Reiss, A. Thomas, R. Gross, and S. T. B. Goennenwein, Phys. Rev. Lett. **108**, 106602 (2012).

[7] T. Janda, J. Godinho, T. Ostatnicky, E. Pfitzner, G. Ulrich, A. Hoehl, S. Reimers, Z. Soban, T. Metzger, H. Reichlova, V. Novak, R. P. Campion, J. Heberle, P. Wadley, K. W. Edmonds, O. J. Amin, J. S. Chauhan, S. S. Dhesi, F. Maccherozzi, R. M. Otxoa, P. E. Roy, K. Olejnik, P. Nemec, T. Jungwirth, B. Kaestner, and J. Wunderlich, Phys. Rev. Mater. **4**, 094413 (2020).

[8] L. Liu, O. J. Lee, T. J. Gudmundsen, D. C. Ralph, and R. A. Buhrman, Phys. Rev. Lett. **109**, 096602 (2012).

[9] D. Wei, M. Obstbaum, M. Ribow, C. H. Back, and G. Woltersdorf, Nat. Commun. **5**, 3768 (2014).

[10] J. Sinova, S. O. Valenzuela, J. Wunderlich, C. H. Back, and T. Jungwirth, Rev. Mod. Phys. **87**, 1213 (2015).

[11] C. H. Li, O. M. J. van 't Erve, J. T. Robinson, Y. Liu, L. Li, and B. T. Jonker, Nat. Nanotechnol. **9**, 218 (2014).

[12] J. Tian, I. Childres, H. Cao, T. Shen, I. Miotkowski, and Y. P. Chen, Solid State Commun. **191**, 1 (2014).

[13] K. Kondou, R. Yoshimi, A. Tsukazaki, Y. Fukuma, J. Matsuno, K. S. Takahashi, M. Kawasaki, Y. Tokura, and Y. Otani, Nat. Phys. **12**, 1027 (2016).

[14] P. Li, W. Wu, Y. Wen, C. Zhang, J. Zhang, S. Zhang, Z. Yu, S. A. Yang, A. Manchon, and X. xiang Zhang, Nat. Commun. **9**, 3990 (2018).

[15] K. Ando, S. Takahashi, K. Harii, K. Sasage, J. Ieda, S. Maekawa, and E. Saitoh, Phys. Rev. Lett. **101**, 036601 (2008).

[16] L. Liu, T. Moriyama, D. C. Ralph, and R. A. Buhrman, Phys. Rev. Lett. **106**, 036601 (2011).

[17] V. E. Demidov, S. Urazhdin, E. R. J. Edwards, and S. O. Demokritov, Appl. Phys. Lett. **99**, 172501 (2011).

[18] O. Mosendz, V. Vlaminck, J. E. Pearson, F. Y. Fradin, G. E. W. Bauer, S. D. Bader, and A. Hoffmann, Phys. Rev. B **82**, 214403 (2010).

[19] F. D. Czeschka, L. Dreher, M. S. Brandt, M. Weiler, M. Althammer, I. M. Imort, G. Reiss, A. Thomas, W. Schoch, W. Limmer, H. Huebl, R. Gross, and S. T. B. Goennenwein, Phys. Rev. Lett. **107**, 046601 (2011).

[20] A. Azevedo, L. H. Vilela-Leão, R. L. Rodríguez-Suárez, A. F. L. Santos, and S. M. Rezende, Phys. Rev. B **83**, 144402 (2011).

[21] M. Obstbaum, M. Härtinger, H. G. Bauer, T. Meier, F. Swientek, C. H. Back, and G. Woltersdorf, Phys. Rev. B **89**, 060407 (2014).

[22] W. Zhang, W. Han, X. Jiang, S.-H. Yang, and S. S. P. Parkin, Nat. Phys. **11**, 496 (2015).

[23] Y. K. Kato, Science **306**, 1910 (2004).

[24] J. Sinova, D. Culcer, Q. Niu, N. A. Sinitsyn, T. Jungwirth, and A. H. MacDonald, Phys. Rev. Lett. **92**, 126603 (2004).

[25] T. Jungwirth, J. Wunderlich, and K. Olejník, Nat. Mater. **11**, 382 (2012).

[26] P. Riego, S. Vélez, J. M. Gomez-Perez, J. A. Arregi, L. E. Hueso, F. Casanova, and A. Berger, Appl. Phys. Lett. **109**, 172402 (2016).

[27] C. Stamm, C. Murer, M. Berritta, J. Feng, M. Gabureac, P. M. Oppeneer, and P. Gambardella, Phys. Rev. Lett. **119**, 087203 (2017).

[28] A. Pattabi, Z. Gu, J. Gorchon, Y. Yang, J. Finley, O. J. Lee, H. A. Raziq, S. Salahuddin, and J. Bokor, Appl. Phys. Lett. **107**, 152404 (2015).

[29] R. Kukreja, S. Bonetti, Z. Chen, D. Backes, Y. Acremann, J. Katine, A. Kent, H. Dürr, H. A. Ohldag, and J. Stöhr, Phys. Rev. Lett. **115**, 096601 (2015).

[30] P. Seifert, K. Vaklinova, S. Ganichev, K. Kern, M. Burghard, and A. W. Holleitner, Nat. Commun. **9**, 331 (2018).

[31] Y. Liu, J. Besbas, Y. Wang, P. He, M. Chen, D. Zhu, Y. Wu, J. M. Lee, L. Wang, J. Moon, N. Koirala, S. Oh, and H. Yang, Nat. Commun. **9**, 2492 (2018).

[32] Y. Liu, Y. Liu, M. Chen, S. Srivastava, P. He, K. L. Teo, T. Phung, S.-H. Yang, and H. Yang, Phys. Rev. Appl. **12**, 064046 (2019).

[33] L. You, R. C. Sousa, S. Bandiera, B. Rodmacq, and B. Dieny, Appl. Phys. Lett. **100**, 172411 (2012).

[34] M. Haertinger, C. H. Back, S.-H. Yang, S. S. P. Parkin, and G. Woltersdorf, J. Phys. D **46**, 175001 (2013).

[35] X. L. Zeng, Y. Liu, Y. Zhang, J. Wu, S. B. Zhu, and Y. H. Chenf, Opt. Express **30**, 2089 (2022).

[36] See Supplemental Material at http://link.aps.org/supplemental/10.1103/PhysRevB.106.174420 for methods and additional experimental results of the signal dependence on laser power, current amplitude, and PEM retardation amplitude. In addition, a description of laser intensity modulation is provided and the mechanism for dynamical PEM induced laser focal spot shifts is discussed.

[37] E. Sagasta, Y. Omori, M. Isasa, M. Gradhand, L. E. Hueso, Y. Niimi, Y. C. Otani, and F. Casanova, Phys. Rev. B **94**, 060412(R) (2016).

[38] M.-H. Nguyen, D. C. Ralph, and R. A. Buhrman, Phys. Rev. Lett. **116**, 126601 (2016).

[39] W. Zhang, V. Vlaminck, J. E. Pearson, R. Divan, S. D. Bader, and A. Hoffmann, Appl. Phys. Lett. **103**, 242414 (2013).

[40] M. Isasa, E. Villamor, L. E. Hueso, M. Gradhand, and F. Casanova, Phys. Rev. B **91**, 024402 (2015).